EISSN: 2707-0425

East African Journal of Science, Technology and Innovation, Vol. 3 (Special issue): February 2022

Optimization of the eccentricity of the pyriform diagram for balancing electrical power systems loading

[1,3,*]ASEMOTA G N O., [1,2]IJUMBA N M

[1]African Centre of Excellence in Energy for Sustainable Development, University of Rwanda, Kigali
[2]School of Engineering, University of KwaZulu-Natal, Durban, South Africa
[3]Morayo College, Nairobi, Kenya

Corresponding author: asemotaegno@gmail.com

Abstract

Electricity is a vital resource need in any modern society for an enhanced lifestyle. Furthermore, electricity load management covers optimal power generation, transmission, distribution, and utilization. Also, demand-side management is electricity consumption beyond the meter, and the ever-increasing electricity demand because of rising population and higher standards of living place a limitation and a constraint on its accessibility to all the citizens in any community. The eccentricity of the pyriform scatter diagram data shape was used to characterize the statistical distribution of the electricity consumption data points around a common axis. The Markov process, the Jordan Canonical transformation, and the Martingales were used to generalize the independent electricity consumption to depend only on the outcome preceding it and not after it. The results show a balanced light loading of 50.0%. The pyriform was symmetrical, convex, and even about the midpoint, which served as the globally optimized solution of the electricity consumption balanced loading problem. A balanced electrical power system loading enables utilities to supply more customers, increases operational efficiencies, and places less stress on electricity generators, transmission, and distribution networks. It is recommended that optimization of electrical power systems loading will lead to energy efficiency, energy savings, lower-cost operations for reliable and sustainable supply, growth, and development. Balanced light loading of electrical power systems components facilitates optimal unit commitment at lower economic and social costs. Whenever service taxes are reduced because of cheaper electricity prices, utilities witness flatter load curves and avoided production costs across power systems operations. This further, lessens blackouts and extends life of utility facilities.

Keywords: *Balanced and light loading; energy efficiency; energy savings; Markov process; Martingales*

Received: 28/10/21
Accepted: 13/12/21
Published: 16/12/22

Cite as: *Asemota and Ijumba, (*2022) Optimization of the eccentricity of the pyriform diagram for balancing electrical power systems loading. East *African Journal of Science, Technology and Innovation 3(Special Issue).*

Introduction

Electricity load management (ELM) is used to control optimal power systems generation, transmission, distribution, and utilisation. Many scholars associate demand-side management

(DSM) with ELM, but supply-side management (SSM) is included in ELM and should be considered for optimisation. This is so because inadequate energy resource optimisation at generation leads to poor power delivery down the value chain. These factors can cause large-scale inefficiencies, unstable grids, and incessant power failures that inconvenience the ultimate electricity consumer. Therefore, energy consumption increases, energy savings mechanisms with rising population, and quality of life directly impact electricity consumption of households (Kerr *et al.,* 2017; Eid *et al.,* 2016; Bimenyimana *et al.,* 2018; Shiraki *et al.,* 2016).

Furthermore, DSM is associated with energy consumption after the electricity meter. It comprises government policies to control energy consumption for environmental sustainability, internal power security and social cohesion, demand response, and reduction of carbon footprint that could negatively impact climate change (Simoes *et al.,* 2017; Warren, 2018).

A pyriform (pear-shaped) diagram is shown to be in hydrostatic stability when the flow velocity of the fluid is constant. In electrical power systems, it occurs when external force like power is balanced by pressure gradient force, which is symmetrically rounded to an ellipsoid. It is a satisfactory approximation to flow speeds when acceleration is negligible. In astrophysics, the field compresses a star under gravitation to the most compact pyriform shape when the angular velocity is much greater than the critical angular velocity. Coincidentally, the shapes aside from the pyriform are unstable (Wu and Karunamuni, 2014; Betterexplained, n.d.).

A pyriform scatter diagram is used to evaluate the correlation between two variables and predicts the behaviour of the dependent variable based on the measurement of the independent variable. The independent variable acts as the control because it influences the behaviour of the dependent variable. It is useful if one variable exhibits quantifiable change and the other does, not. It is also, the best approach to indicate nonlinear patterns because association points can either fall on a line or a curve as in the pyriform (Usmani, 2020).

However, the drawbacks of the scatter diagrams are that they do not provide the exact extent of correlation between variables. Also, they do not indicate the quantitative measurements of the association between variables nor indicate the associations beyond two variables.

In addition, the eccentricity of data shapes is used to characterise a statistical distribution of data points around a common axis. Eccentricity is interpreted as the fraction of the distance along the semi-major axis in which lies the focus. Eccentricity also ranges from 0 to infinity and the greater the eccentricity, the less the conic section resembles a circle (Lane and Ziemer, n.d.). Eccentricity is a measure of the deviation from being circular. It also measures how closely a conic resembles a circle. For any conic section, eccentricity is the condition of being eccentric (abnormal or irregular). It is equally the constant ratio of the distance from the directrix (a fixed-line) (Robinson, 2018; Kirkpatrick *et al.,* 1983).

The objective of the study was to investigate how the eccentricity of the pyriform (pear-shaped) of the reduced electricity consumption pattern of a utility in Namibia can be used to balance electrical power systems loading.

Materials and Methods

A group of expert judges like electrical engineers, economists, and planners was used to validate a 5-point Likert scale residential electricity load management questionnaire used to gather survey data for statistical analysis in Windhoek City, Namibia. Out of the over 300 self-report questionnaires randomly distributed in Windhoek, Namibia, only 127 responses were returned. The sample size adequacy was proven in (Asemota, 2014). The statistical analysis yielded a pyriform (pear-shaped) of the reduced electricity consumption pattern that was subsequently subjected to eccentricity analysis, Markov process, Jordan canonical transformation, and the Martingales for balanced electrical power systems loading.

Eccentricity of the Pyriform

Lines were drawn along and across the major and minor axes of the pyriform in Figure 1 and

measurements were taken as shown in Figure 2. Other tangent lines were also drawn to obtain angular measurements of the data points on the bimodal pyriform. The ratios between the major and minor axes lengths were used to obtain the eccentricities because the pyriform can be approximated to an ellipsoid.

The eccentricity e, is determined as (Robinson, 2018; Fun, n.d.; Weisstein, n.d.; Page, 2011):
For an ellipse, the length of the minor axis is:
For an ellipse, the length of the minor axis is:
$\sqrt{(a+b)^2 - f}$ (1)
where f is the distance between foci, a, b are the distances from each focus to any point on the ellipse.

The length of the major axis is:
$a + b$ (2)
where a, b were as earlier defined. Therefore:
$e = \frac{c}{a}$ (3)
where c is the distance from the centre of the conic section to the focus. Also,
$e = \sqrt{1 + \frac{b^2}{a^2}} = \frac{c}{a}$ (4)
For a hyperbola: $\left(e = \frac{c}{a} > 1\right)$; for a parabola: $(e = 1)$; for an ellipse: $(e < 1)$; for a circle: $(e = 0)$.
In addition, the eccentricity can also be calculated as (Fun, n.d.):
$e = \frac{\sin\beta}{\sin\alpha}$ (5)

where: $0 < \alpha < 90^0$; $0 < \beta < 90^0$.

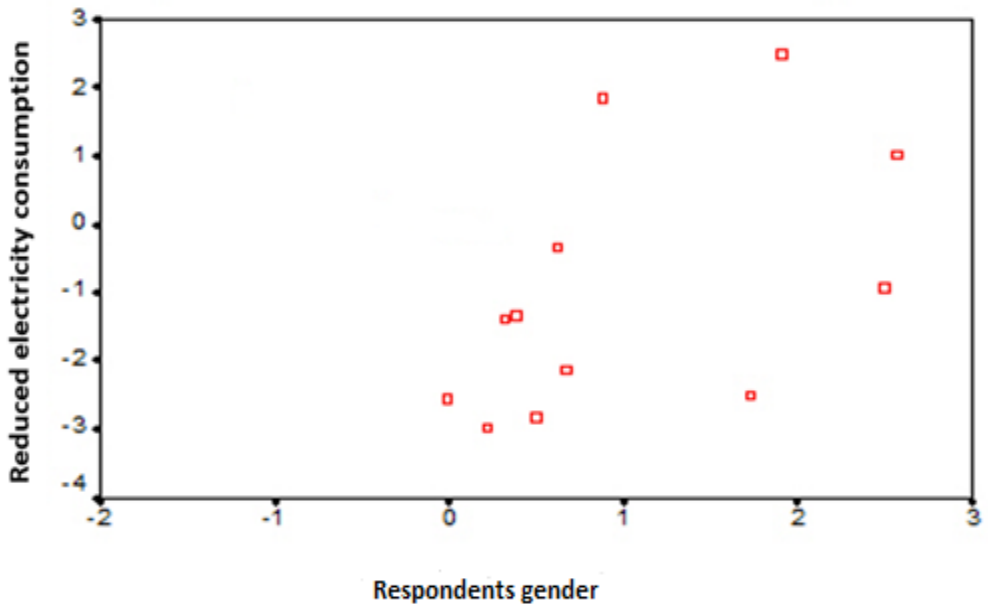

Figure 1. Scatter plot: Reduced electricity consumption pyriform (Asemota, 2013)

The determination of various eccentricities for the pyriform scatter diagrams are:
$e_1 = \frac{c}{a} = \frac{6.7\ cm}{4.8\ cm} = 1.396$; $e_2 = \frac{\sin 62^0}{\sin 40^0} = \frac{0.88294759285}{0.64278760968} = 1.374$;
$e_3 = \frac{\sin 70^0}{\sin 40^0} = \frac{0.9396922078}{0.64278760968} = 1.462$; $e_4 = \frac{\sin 28^0}{\sin 40^0} = \frac{0.46947156278}{0.64278760968} = 0.730$;
$e_5 = \frac{\sin 77^0}{\sin 40^0} = \frac{0.97437006478}{0.64278760968} = 1.516$; $e_6 = \frac{\sin 45^0}{\sin 40^0} = \frac{0.70710678118}{0.64278760968} = 1.100$;
$e_7 = \frac{\sin 65^0}{\sin 40^0} = \frac{0.90630778703}{0.64278760968} = 1.410$; $e_8 = \frac{\sin 83^0}{\sin 40^0} = \frac{0.99254615164}{0.64278760968} = 1.544$.

Mainly because the eccentricities calculated above were all almost greater than unity, it can be partially concluded that the pyriform (pear-shaped) scatter diagram is a hyperbola. A hyperbola is a smooth curve lying in a plane, which is defined by its geometric properties or by equations that form its solution set (Mathwarehouse, n.d.). Also, and because there was one of the eccentricities ($e_4 < 1 \approx 0.730$) less than unity, the pyriform scatter diagram can be best described as a platykurtic ellipsoidal bimodal pyriform. This is so because, there was a small tail, a dimple, two lobes, and an outer curve representing an ellipsoid (not shown, but can be gleaned from the shape of the pyriform).

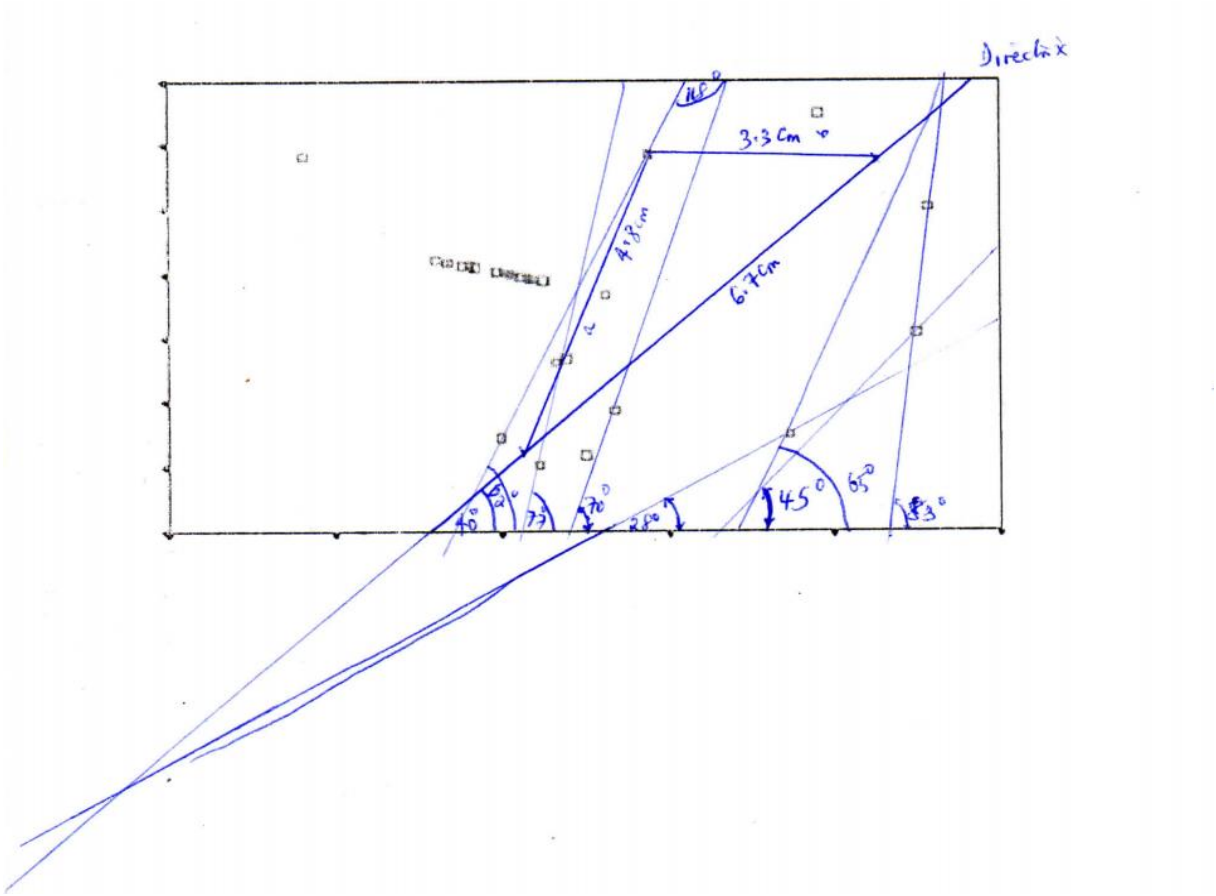

Figure 2. Eccentricity measurement lines for the reduced electricity consumption pyriform

Markov Process

Markov processes are the simplest generalisations of independent processes. They permit the outcome at any instant to depend only on the outcome preceding it and none before that. In a Markov chain, the system can occupy a finite or countably infinite number of states $e_1, e_2, \dots, e_k$. The future evolution of the process depends only on the present and not how it arrived at that state. A stochastic process is a non-countable infinity of random variables, one for each t (Papoulis & Pillai, 2008). The equation of the pyriform is (McGraw-Hill & Parker, 2003):

$$y = -ax^4 + bx^3 \quad (6)$$

Classification of states

$$\begin{pmatrix} -ax^4 & 0 & 0 & 0 & 0 \\ 0 & bx^3 & 0 & 0 & 0 \\ 0 & 0 & 0 & 0 & 0 \\ 0 & 0 & 0 & 0 & 0 \\ 0 & 0 & 0 & 0 & 0 \end{pmatrix} \quad (7)$$

For given states e_k and e_l, if the probability $P_{kl}^{(n)} > 0$, for some n, there is a positive probability of getting to e_l starting from e_k in n steps. Hence, the state e_l is accessible from e_k. If e_k and e_l are

accessible from each other, then e_k communicates with e_l. If every Markov state is accessible from every other state, in many transitions, then it is an irreducible communicating chain (Papoulis and Pillai, 2008; Patil *et al.*, 2012).

For the 5×5 pyriform transition matrix,

$$Q = \begin{pmatrix} a_{11} & 0 & 0 & 0 & 0 \\ 0 & a_{22} & 0 & 0 & 0 \\ 0 & 0 & 0 & 0 & 0 \\ 0 & 0 & 0 & 0 & 0 \\ 0 & 0 & 0 & 0 & 0 \end{pmatrix} \quad (8)$$

where $a_{kl} > 0$ are positive probabilities. But a_{11} and a_{22} are the only nonzero entries in rows 1 and 2. By the Jordan canonical transformation, $a_{11} \equiv 1$ and $a_{22} \equiv 1$. Therefore, e_1 and e_2 are absorbing states. This is so because, both e_1 and e_2 are closed sets on themselves. They also communicate with each other, as irreducible communicating chains (Papoulis and Pillai, 2008; Patil *et al.*, 2012). In addition, $Q_1 = a_{11}, Q_2 = a_{22}, Q_3 = 0, Q_4 = 0$

$$Q_4 \triangleq [W, X] = 0 \quad (9)$$

$$\begin{pmatrix} 1 & 0 & 0 & 0 & 0 \\ 0 & 1 & 0 & 0 & 0 \\ 0 & 0 & 0 & 0 & 0 \\ 0 & 0 & 0 & 0 & 0 \\ 0 & 0 & 0 & 0 & 0 \end{pmatrix} \begin{pmatrix} -ax^4 \\ bx^3 \\ 0 \\ 0 \\ 0 \end{pmatrix} \quad (10)$$

Whenever the row sums and column sums are each unity, the transition matrix Q, is termed a doubly stochastic matrix. Therefore, the pyriform is an irreducible doubly stochastic communicating Markov chains with two absorbing states.

Martingales

A Markov chain is a martingale if for every k, the expectation of the probability distribution $\{q_{kl}\}$ equal k. Hence, in a martingale

$$\sum_l l q_{kl} = k \quad (11)$$

Let $e_0, e_1, \dots, e_N$ be states in a martingale, with $k = 0$ and $k = N$ in (11), we have

$q_{00} = q_{NN} = 1$.

Thus, e_0 and e_N are absorbing states. If we assume these to be persistent states in the chain, then $e_1, e_2, \dots, e_{N-1}$ are transient states (Papoulis & Pillai, 2008). The system is finally absorbed into e_0 or e_N. From (11), and by induction, we have

$$\sum_l^N h q_{lh}^{(n)} = l \quad (12)$$

for all n.

From the above equation (12), the expectation value becomes

$E\{\mathbf{x}_{n+m}|\mathbf{x}_m\} = \mathbf{x}_m$ for all n and m.

This is the definition of a martingale (Papoulis and Pillai, 2008).

Also, $q_{lh}^{(n)} \to 0$ for every transient state e_h, $h = 1,2, \dots, N-1$, for $l > 0$ in (12). Substituting appropriate values into (12) gives the only solution

$$q_{lN}^{(n)} \to \frac{l}{N} \quad (13)$$

Simply because there are only two absorbing states in the pyriform, we obtain

$$q_{l.0}^{(n)} \to 1 - \frac{l}{N} \quad (14)$$

If the system starts with e_l, the probability of the final absorption into e_0 and e_N are $1 - \frac{l}{N}$ and $\frac{l}{N}$, respectively (Papoulis and Pillai, 2008). If all states are equally likely, to begin with, then the probability of the final absorption into e_N is

$$\lim_{n\to\infty} \sum_{l=0}^N q_l^{(0)} q_{l,N}^{(n)} = \sum_{l=1}^N \frac{1}{N+1} \cdot \frac{l}{N} = ½ \quad (15)$$

Therefore, for a randomly chosen initial distribution, the final absorption into either e_0 or e_N are both equally likely events for a finite state of the martingale (Papoulis and Pillai, 2008).

For the pyriform absorbing states, only a_{11} and a_{22} are admissible states. Regardless of the model formulation procedure, and beginning from an initial state e_l, the final absorption probabilities into e_0 and e_N are $1 - \frac{l}{N}$ and $\frac{l}{N}$, respectively.

Whenever this procedure is likened to breeding in genetics, only absorbing states (pure breeds) are allowed, while mixed breeds gradually go extinct (Papoulis and Pillai, 2008).

Therefore, the probability of the final absorption into either a_{11} or a_{22} of the pyriform absorbing states is a half (0.5). This is also the optimal (best) solution to the pyriform electrical power systems balanced loading problem under investigation in this study. It also perfectly agrees with the Quetelet curve optimisation solution of the mid-point percentile (0.5) using the multivariate approach (Papoulis & Pillai, 2008; Jahoda, 2015). It was also found to be a convex set (Bishop, 2008;

Asemota, 2009). This local optimum was equal to the global optimum in the interval of convexity.

Results

The eccentricities of the reduced electricity consumption pyriform were 1.396, 1.374, 1.462, 0.730, 1.516, 1.100, 1.410, and 1.544, respectively. Therefore, the pyriform scatter diagram can be best described as a platykurtic ellipsoidal bimodal pyriform. This is so because, there was a small tail, a dimple, two lobes, and an outer curve representing an ellipsoid (not shown, but can be gleaned from the shape of the pyriform). Also, the reduced electricity consumption pyriform is an irreducible doubly stochastic communicating Markov chains with two absorbing states. Above all, the probability of the final absorption into either a_{11} or a_{22} of the reduced electricity consumption pyriform absorbing states is a half (0.5). This is also the optimal (or best) solution to the pyriform electrical power systems balanced loading problem in this study. The quantity of information we receive from a random variable depends on the amount of "surprise" we learn from the value. Thus, a less probable event contains more information than a very likely event. This is so because the certainty of an event occurring has no information content. Hence, the measure of the information content depends on the monotonic probability distribution function. Also, the information received is the sum of the information received from each of the events separately. If there are relatively fewer scores in the tails of the pyriform, the shape is platykurtic, otherwise, it is leptokurtic. If the distribution has short tails, it is platykurtic, because the distribution differs in kurtosis. Furthermore, the eccentricity of data shapes describes the statistical distribution of data points around a common axis. Eccentricity is interpreted as the fraction of the distance along the semi-major axis in which lies the focus. Eccentricity also ranges from 0 to infinity and the greater the eccentricity, the less the conic section resembles a circle. Eccentricity is a measure of the deviation from being circular. It also measures how closely a conic resembles a circle. For any conic section, eccentricity is the condition of being eccentric (abnormal or irregular). It is equally the constant ratio of the distance from the directrix (or a fixed line). In addition, if every Markov state is accessible from every other state, in a number of transitions, then it is an irreducible communicating chain.

Discussion

The pyriform (Figure 1) of the scatter diagram has a bimodal distribution because it has two peaks. If there are relatively fewer scores in its tails, the shape is platykurtic, otherwise, it is leptokurtic. If the distribution has short tails, it is platykurtic, because the distribution differs in kurtosis (Lane and Ziemer, n.d.). If e_k and e_l are accessible from each other, then e_k communicates with e_l. This is so because both e_k and e_l are closed sets on themselves. If every Markov state is accessible from every other state, in many transitions, then it is an irreducible communicating chain (Papoulis & Pillai, 2008; Patil *et al.,* 2012). Whenever the row sums and column sums are each unity, the transition matrix Q, is termed a doubly stochastic matrix (Papoulis and Pillai, 2008). Therefore, the reduced electricity consumption pyriform is an irreducible doubly stochastic communicating Markov chain with two absorbing states. A half $(1/2)$ is also the optimal and best solution to the pyriform electrical power systems balanced loading problem under investigation in this study. It also perfectly agrees with the Quetelet curve optimisation solution of the mid-point percentile (0.5) using the multivariate approach (Papoulis & Pillai, 2008; Jahoda, 2015). It was also found to be a convex set. This local optimum is equal to the global optimum in the interval of convexity (Bishop, 2008; Asemota, 2009). The fifty percent average electrical power systems loading achieve optimal or balanced loading without hotspots or localised heating. Further, any local optimum is also a global optimum, provided the constraints define a convex region. Also, these optimisation results describe linear functionals (Bishop, 2008), where the gradient indicates the direction of the greatest change along the line of equipotential or equal energy (Betterexplained, n.d.). The reduced electricity consumption pyriform optimisation is necessary for electricity network expansion planning because the utility can supply more electricity consumers. Also, the transmission lines infrastructure can evacuate rising electricity generation and consumption capacities because of average and balanced

loading. Balanced electrical power systems loadings can support, enhance, and strengthen optimal power systems operators' responses in emergencies (Asemota, 2012; Hu *et al.,* 2016). Electrical power systems balanced loading increase and maximise cost-benefit ratios, which enhance reliability improvements, reduce operational costs against initially high optimal power generation, transmission, and distribution investments. Further, to minimise total investment costs, transmission lines losses, and optimally and efficiently engage electricity production units that satisfy future load growth having additional security and operational constraints (Asemota, 2012; Hu *et al.,* 2016). In addition, the Quetelet index is used to create awareness, education, and behaviour modification especially among the average citizens on energy efficiency for affordable, reliable, and sustainable electricity supply (Asemota and Ijumba, *in press*).

Conclusion

The reduced electricity consumption pyriform optimisation is necessary for electricity network expansion planning because the utility can supply more electricity to consumers. Also, the transmission lines infrastructure can evacuate rising electricity generation and consumption capacities because of average and balanced loading. Balanced electrical power systems loadings can support, enhance, and strengthen optimal power systems operators' responses in emergencies. Electrical power systems balanced loading increase and maximise cost-benefit ratios, which enhance reliability improvements, reduce operational costs against initially high optimal power generation, transmission, and distribution investments. Further, to minimise total investment costs, transmission lines losses, and optimally and efficiently engage electricity production units that satisfy future load growth having additional security and operational constraints. In addition, the Quetelet index is used to create awareness, education, and behaviour modification especially among the average citizens on energy efficiency for affordable, reliable, and sustainable electricity supply.

Also, the 50.0% or balanced electrical power systems loading proposed in this study could lead to a change in plant stock, increase base power plants, and reduce peaking power plants, tariffs, and fuel costs. Higher combustion efficiency and higher sunk capital costs could lead to reduced capacity costs, with costs spread across greater units of output. Other benefits include reduced transmission and distribution charges; retail costs of goods and services; service taxes; and gains from flatter load curves and avoided production costs across power systems operations.

Acknowledgment

This work was carried out in the African Centre of Excellence in Energy for Sustainable Development, University of Rwanda, Kigali, Rwanda.

References

Asemota, G. N. O. (2009). On a class of computable convex functions, *Canadian Journal of Pure and Applied Sciences, 3*(3), 959-965.

Asemota, G. N. O. (2012). Optimal two-way conductor design using computable convex functions approach, *Advances in Materials Research, 367,* 75-81.doi:10.4028/www.scientific.net/AMR.367.75

Asemota, G. N. O. (2013). *Electricity Use in Namibia*. Indiana: iUniverse.

Asemota, G. N. O. (2014). Communality performance assessment of electricity load management model for Namibia, *IEEE-AIMS 2nd International Conference on Artificial Intelligence, Modelling and Simulation*. (pp. 252-257). New Jersey: IEEE.

Asemota, G. N. O., & Ijumba, N. M. (in press). Using blinds, day-lighting, and geyser temperature settings to reduce electricity consumption and pricing patterns in energy-efficient buildings, *Journal of South African Institute of Electrical Engineers*.

Betterexplained. (n.d.). Vector calculus: Understanding the gradient- better Explained. Retrieved from: https//betterexplained.com/articles/ve

ctor-calculus-understanding-the-gradient/

Bimenyimana, S., Ishimwe, A., Asemota, G. N. O., Kemunto, C. M., & Li, L. (2018). Web-based design and implementation of smart home appliances control system. (pp. 1-9). *IOP Conference Series: Earth Environmental Science, 168*.

Bishop, C. M. (2008). *Pattern recognition and machine learning*. Singapore: Springer.

Eid, C., Bollinger, A. L., Koirala, B., Scholten, D., Facchinetti, E., Lilliestan, J., & Hakvoort, R. (2016). Market integration of local energy systems: Is local energy management compatible with European regulation for retail competition? *Energy, 114,* 913-922.

Fun, T. P. (n.d.). Bisection of the eccentricity. National University of Singapore. Retrieved from: www.math.nus.edu.sg/aslaksen/projects/tpf.pdf.

Hu, Y., Bie, Z., Ding, T., & Lin, Y. (2016) An NSGA-II based multi-objective optimization for combined gas and electricity network expansion planning, *Applied Energy*, *167*, 280-293.

Jahoda, G. (2015). Quetelet and the emergence of the behavioral sciences, *SpringerPlus, 4*, 473. Retrieved from: https://www.ncbi.nlm.nih.gov/pmc/articles/PMC4559562/

Kerr, N., Gouldson, A., & Barret, J. (2017). The rationale for energy efficiency policy: Assessing the recognition of the multiple benefits of energy efficiency retrofit policy. *Energy Policy*, *106*, 212-221.

Kirkpatrick, E. M., Schwarz, C. M., Davidson, G. W., Seaton, M. A., Simpson, J., & Sherrard, R. J. (1983). Chambers 20th Century Dictionary. Edinburgh: Chambers.

Lane, D. M., & Ziemer, H. (n.d.). Chapter 1: Introduction section-Distributions. Retrieved from:Onlinestatbook.com/2/introduction/distributions.html.

Mathwarehouse.com. (n.d.) Hyperbola. Retrieved from: https://www.mathwarehousecom/hyperbola/graph-equation-of-a-hyperbola.php

McGraw-Hill., & Parker, S. P. (2003). *McGraw-Hill dictionary of scientific and technical terms* (6th ed.). New York: McGraw-Hill.

Page, J. (2011). Major/minor axes of an ellipse. Retrieved from: https:/www.mathopen.ref.coin/ellipse axes.html

Papoulis, A., & Pillai, S. U. (2008). *Probability, random variables and stochastic processes* (4th ed.). New Delhi: Tata McGraw-Hill.

Patil, S., Nagaraju, P., & Deasi, S. (2012). Study of the behavior models based on probability and time using Markov process and transition. *International Journal of Computer Science&Engineering, 4*(3), 512-521. Retrieved from: www.enggjournals.com/ijcse/doc/IJCSE12-04-018.pdf

Robinson, A. (2018). How to calculate eccentricity. Retrieved from: https://sciencing.com.com/how-to-calculate-eccentricity-12751764.html

Shiraki, H., Nakamura, S., Ashina, S., & Honjo, K. (2016). Estimating the hourly electricity profile of Japanese households-Coupling of engineering and statistical methods. *Energy, 114,* 478-491.

Simoes, S., Nijs, W., Ruiz, P., Sgobbi, A., & Thiel, C. (2017). Comparing policy routes for low-carbon power technology deployment in EU-an energy systems analysis. *Energy Policy, 101*, 353-365.

Usmani, F. (2020). What is a Scatter Diagram [A Correlation Chart?]. PM Study Circle. Retrieved from: https://pmstudycircle.com

Warren, P. (2018). Demand-Side Policy: Global evidence base and implementation patterns. *Energy & Environment, 0*(0), 1-26.

Weisstein, E W. (n.d.). Eccentricity. mathworld-A wolfram web resource. Retrieved from: http://mathworld.woffram.com/Eccentricty.html

Wu, J., & Karunamuni, R. J. (2014). Profile Hellinger distance estimation statistics. *Journal of Theory & Applied Statistics.* doi: 10.1080/02331888.2014.946928